Polymer Journal (2021) 53:765–777
https://doi.org/10.1038/s41428-021-00479-x

FOCUS REVIEW

A benchmark for gel structures: bond percolation enables the fabrication of extremely homogeneous gels

Xiang Li[1]

Received: 26 January 2021 / Revised: 24 February 2021 / Accepted: 25 February 2021 / Published online: 14 April 2021

Abstract

Gels are soft-elastic materials consisting of a three-dimensional crosslinked polymer network and liquid filling the space between this network. Numerous gels with unique physical properties have been synthesized and are widely used in our daily lives. However, all of these gels contain a substantial level of structural defects, as detected by scattering measurements. Despite the tremendous efforts made in recent decades to remove imperfections from gels, discernible signs of spatial defects have been persistently observed in gels. Researchers believe that gels are inherently heterogeneous. In this focus review, I briefly introduce a recent finding from our research group's efforts to fabricate polymer gels free of spatial heterogeneities. The commonly observed scattering profiles for the spatial defects disappeared in the homogeneous gels. The newly observed scattering profiles are a benchmark for gel structures.

Introduction

Gels are soft-elastic materials used in various applications, spanning from cutting-edge biomedical applications and electronic devices to food industries [1–7]. The unique physical behaviors of gels, such as high deformability [8, 9], solvent retaining capability [10–12], size filtration effects [13–15], and volume phase transition behaviors [16–18], originate from their three-dimensional polymer networks [19, 20]. The gels are synthesized by crosslinking polymer chains dissolved in a solvent [19, 21–25]; in some cases, polymerization and crosslinking occur simultaneously [26, 27]. The developed three-dimensional crosslinked polymers eventually percolate the whole solution and change the system from a fluid "sol" to a solid "gel" [20, 24, 28, 29]. Because the polymer chains continually fluctuate in the solution [30–32], the crosslinking reaction tends to result in a complicated network with substantial defects [33, 34], including dangling ends, loops, entanglements, and nonuniform crosslinker distribution. These defects cause weak mechanical properties [35], low transparency [36], and abnormal swelling/deswelling behavior [37], which limits the understanding of gel physics and the applications of the gels. Quantifying the defects is challenging because no technique can directly observe the *raw* polymer network in real space with sufficient temporal/spatial resolutions along with an acceptable signal-to-noise ratio. Therefore, gel network structures have been mostly studied using scattering measurements, such as light, X-ray, and neutron scattering, in Fourier space [16, 17, 23, 38–48]. The scattering profiles provide information about the spatial and temporal correlations between the polymer chains [39, 41, 44, 49–58]. Famous signatures of the spatial defects detected by scattering measurements are fractal small-angle scattering [59, 60], stationary laser speckles [61, 62], and nonergodic dynamics [63, 64], reflecting the nonuniform distribution of polymer chains in the gels, i.e., spatial heterogeneities [46, 65–67]. These unique scattering behaviors have been observed in all polymer gels; therefore, they are often regarded as the criteria of being gels [59–61, 63, 68].

Many attempts have been made to reduce the spatial heterogeneities in gels, such as by synthesizing gels from monodispersed polymer chains [69], using a uniform crosslinking process, such as a photoreaction [70], by limiting unfavorable intramolecular reactions via the A–B type cross-coupling of multiarmed star polymers [71] and even by crosslinking polymer chains with movable crosslinkers that can relax the spatial heterogeneities [72]. Nevertheless, discernible signs of imperfections have always been

✉ Xiang Li
x.li@issp.u-tokyo.ac.jp

[1] Institute for Solid State Physics, The University of Tokyo, Kashiwa, Chiba, Japan

observed in gels [68, 70, 71, 73, 74]. Gels have been believed to be an inherently heterogeneous material.

Our recent study broke this preconception: we presented a simple but universal scheme to fabricate gels with a highly ordered network [22, 75, 76]. Our strategy is to bring a geometric constraint into the pregel solution so that the polymer solution is always uniformly filled with the starting polymer units throughout the gelation reaction. This gelation framework is known as "bond-percolation" in classical percolation theory [29, 77]. The spatial and temporal heterogeneity of the synthesized gel network is investigated in Fourier space using scattering techniques. Our gel did not show any signatures of heterogeneity: no stationary laser speckles, no anomalous small-angle scattering, and fully ergodic concentration fluctuation were observed. These results are entirely different from the widely accepted picture of gels. Surprisingly, both the small-angle scattering profiles and intensity correlation functions of our gels are identical to those of noncrosslinked pregel solutions. In this focus review, I would like to briefly introduce the history of research into gel structures and then present our strategy to vastly reduce heterogeneous structures.

General structures of gels

Fractal small-angle scattering

Figure 1a shows the small-angle X-ray scattering (SAXS) profiles of an alginate gel [78], where alginates were gradually crosslinked with calcium ions in an aqueous solution (Fig. 1b). The scattering intensity $I(q)$ increased at small q values ($q < 0.1$ Å^{-1}) as the crosslinking proceeded, indicating the formation of some large structures in the gels that did not exist in the noncrosslinked alginate solution. q is the magnitude of the scattering vector, which is inversely proportional to the distance in real space. Note that we cannot observe these large structures if their local concentrations

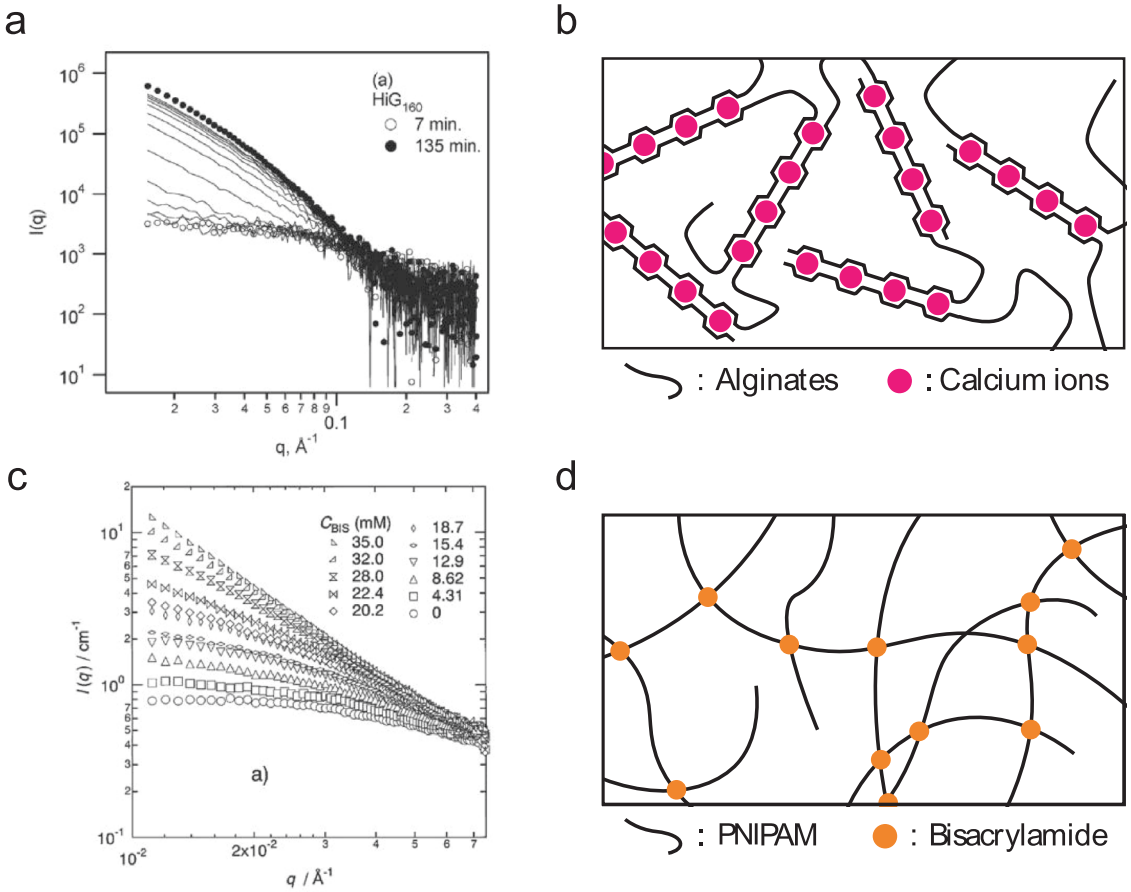

Fig. 1 SAXS and SANS profiles of the conventional gels. **a** SAXS profiles of alginate gels with different crosslinking densities [78]. The crosslinking density of the alginate gel changed over time during the SAXS measurements. Reprinted (adapted) with permission from [78]. Copyright 2003 American Chemical Society. **b** Schematic of alginate gels crosslinked with calcium ions. **c** SANS profiles of poly(*N*-isopropylacrylamide) (PNIPAM) gels with different crosslinking densities [82]. **d** Schematic of PNIPAM gels crosslinked with *N*,*N*′-methylenebisacrylamide (bisacrylamide). The experiments were performed at a temperature below the lower critical solution temperature (LCST) of PNIPAM. Reprinted from [82] with permission from Elsevier

are the same as the surrounding system because there is no scattering contrast between the large structures and the surrounding system. For example, a sizeable dilute polymer cluster dissolved in a semidilute solution of the same polymers is invisible for typical scattering measurements [24, 28, 30, 45]. Therefore, the fractal small-angle scattering profiles in the gels indicate that the observed large structures have a higher or lower local concentration than the surrounding gel network. The apparent fractal dimension D, e.g., $I \sim q^{-D}$, contains both the mass fractal dimension and the size distribution of the heterogeneous structures. The value of D varies widely from 0.5 to 4 [73, 79–81], suggesting the complexity of the gel networks. Figure 1c shows similar scattering profiles for a poly(*N*-isopropylacrylamide) (PNIPAM) gel [82] synthesized by the copolymerization of *N*-isopropylacrylamide (monomers) and bisacrylamide (crosslinkers). The profiles of the PNIAPM gel and the uncrosslinked PNIPAM solution were similar at low crosslinking ratios. However, as more crosslinkers were introduced into the gels, fractal small-angle scattering became more dominant. Fractal small-angle scattering is a common feature of gels. The representative size of the spatial heterogeneity is generally larger than the observation range of general SAXS and SANS instruments (~200 nm). When the structures are smaller than ~1 μm, we can use static light scattering (SLS) to determine the size of the spatial heterogeneity [83]. The swelling of the gels typically induces additional spatial heterogeneity in the gel network that is attributed to connectivity heterogeneity, resulting an enhanced fractal small-angle scattering [84].

Stationary laser speckles

Figure 2a shows a 2D laser speckle image of a polystyrene gel swollen in cyclohexane at a temperature where cyclohexane is a good solvent for polystyrene [85]. The speckle pattern was recorded for an extended period, e.g., 30 s; this is a time period in which polymers typically achieve complete relaxation. Therefore, the maxima and minima of the scattering intensity in the image reflect the nonuniform and time-independent *frozen* distribution of the polymer chains [65, 86]. The frozen components are attributed to the spatial heterogeneities observed in the SAXS and SANS profiles. Note that in typical SAXS and SANS experiments, we do not see these speckles on the 2D scattering profiles because the beam coherence of conventional X-rays and neutrons are insufficient to visualize the speckles. Instead, general SAXS or SANS experiments yield an ensemble-averaged scattering intensity, which corresponds to the spatially averaged intensity of the laser speckle pattern (in a different q-region). Figure 2b shows the 1D laser speckle patterns from a PVA gel [61]. A bifunctional acid, Congo red, physically crosslinked the PVA. The gel is stable at room temperature but changes to a solution at high temperatures due to the dissociation of the Congo red from PVA. 1D speckle patterns were measured by recording the light scattering intensities at 100 different randomly chosen sample positions. The intensity depends strongly on the sample positions, indicating the variety of the local gel networks at each sample position. The laser speckles in PVA gel have weaker fluctuations at high temperatures, suggesting that the gel networks become more uniform. This tendency is attributed to the decrease in the crosslinking density in the PVA gels at higher temperatures. When the PVA gel changed into a solution at 57 °C, the laser speckles disappeared entirely. $\langle I \rangle_E$ in Fig. 2b is the averaged scattering intensity over the 100 sample positions. As explained above, this intensity corresponds to the intensities observed in the SAXS and SANS profiles at the q-range for visible light.

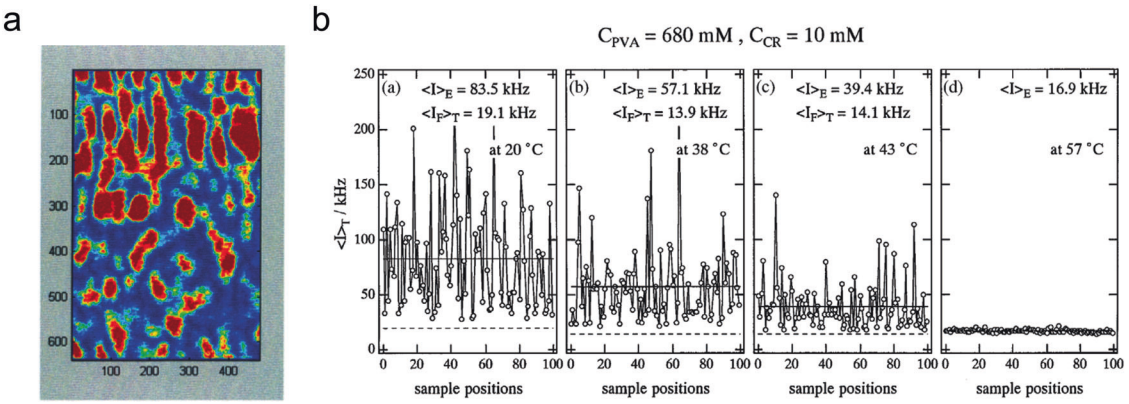

Fig. 2 Laser speckle patterns observed in conventional polymer gels. **a** 2D laser speckle patterns from a polystyrene gel swollen with cyclohexane at 45 °C [85]. Cyclohexane is a good solvent for polystyrene at this temperature. Reprinted (adapted) with permission from [85]. Copyright 2000 American Chemical Society. **b** 1D laser speckle patterns from a polyvinyl alcohol (PVA) gel crosslinked by a sulfonic acid, Congo red, at various temperatures [61]. The association ratio between PVA and Congo red decreases with temperature. Reprinted with permission from [61]. Copyright 1999 by the American Physical Society

Position-dependent relaxation

Figure 3a shows the intensity correlation functions ($g^{(2)}(\tau) - 1$) of a gel during its gelation process, measured by dynamic light scattering (DLS) [87]. τ is the lag time in the correlation functions. As the crosslinking proceeded, two relaxation modes appeared in $g^{(2)}(\tau) - 1$ (curve 2). The fast mode corresponds to the concentration fluctuation, a universal relaxation mode for semidilute polymer solutions and gels. The slow mode shows the translational dynamics of some large heterogeneous structures, whose local polymer concentration is different from the surrounding gel network. As the crosslinking proceeded further (curves 3–5), the relaxation of the slow mode became even slower by a few orders of magnitude, suggesting the growth of large heterogeneities and an increase in the solution viscosity. After the gel was formed (curves 6–7), the value of the intensity correlation function at zero lag time, $g^{(2)}(0) - 1$, greatly decreased, suggesting the appearance of immobilized polymers. It can be slightly difficult to understand, but the immobilized polymers are not the gel network itself but the heterogeneous structures trapped in the gel network. When a spatially homogeneous gel is formed, $g^{(2)}(0) - 1$ does not decrease at the gel point [75]. Although the decrease in $g^{(2)}(0) - 1$ is not directly attributed to the gel network [75], the decrease point matches the gel point [87] because the immobilization of the spatial heterogeneities occurs when the incipient gel network is formed. A similar decrease in $g^{(2)}(0) - 1$ at the gel point was also observed when the nanoparticles were trapped in the gel networks [24, 28], supporting the discussion mentioned above. Note that the formation of immobilized voids [76], i.e., where no polymer chains exist, also leads to decreased $g^{(2)}(0) - 1$ [76]. Figure 3b shows the intensity correlation functions, $G(t) - 1$, in a PNIPAM gel measured at a fixed scattering angle but at four different sample positions, noted with different X values [64]. The notation $G(t) - 1$ is the same with $g^{(2)}(\tau) - 1$. X is the scattering intensity ratio of the dynamic term, I_F/I_T, calculated with $G(0) - 1 = X(2 - X)$ based on the partial heterodyne model. I_F is the intensity from the dynamic term, and I_T is the total scattering intensity [88]. The intensity correlation functions depend strongly on the sample positions, indicating a large variety in the local structures. The observed relaxation on $G(t) - 1$ corresponds to the concentration fluctuation in the gel. The main cause of the variance of $G(t) - 1$ at each sample position is the presence of "frozen" spatial heterogeneities, which differ at each position.

Towards homogeneous gels

A–B type end-crosslinking

Figure 4a shows a gel with a near-ideal network synthesized by end-crosslinking two types of four-armed polyethylene glycols (tetraPEG) with mutual reactive end groups [71]. The combination of the end groups can be NHS to amine [89] or maleimide to thiol [21]. Because A-type tetraPEG can only react with B-type tetraPEG, the intramolecular reaction, i.e., the reaction within the same tetraPEG, should be entirely suppressed in this reaction system. In addition, as the branch point is located at the center of the star polymers, the mesh size of this gel should be highly uniform. Such well-defined structures have enabled precise design and control of the physical properties of gels [90–97]. The SANS profiles of tetraPEG gels show a plateau in the small-angle region up to $q \sim 0.005$ Å^{-1}, indicating the high homogeneity of tetraPEG gels on a length scale smaller than ~100 nm (Fig. 4b) [73]. Because of the high homogeneity of tetraPEG gels, the mechanical properties of tetraPEG gels are also largely improved compared with

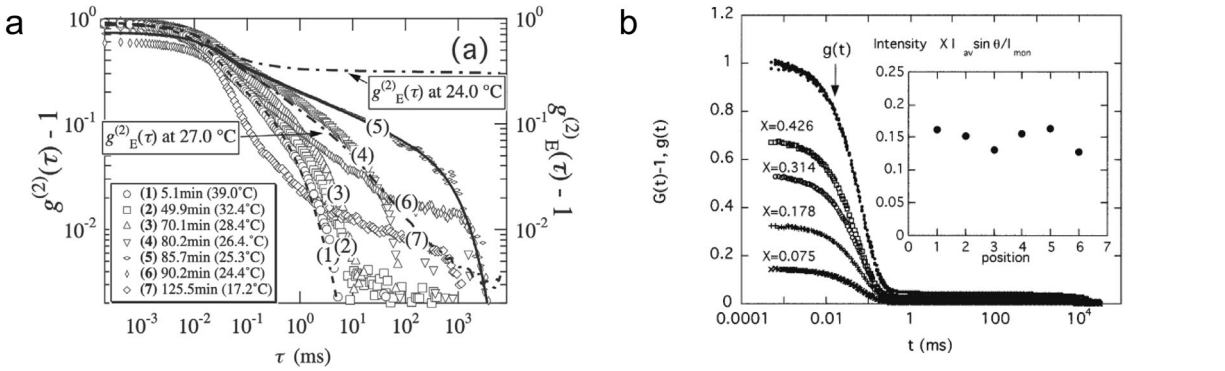

Fig. 3 Dynamics of the polymer chains in conventional gels observed by dynamic light scattering. **a** Polymer dynamics in a gelatin gel during its gelation process [87]. Gelatin is a physical gel that changes from a solution to a gel by decreasing the temperature. The apparent sol–gel transition temperature is ~24 °C. The intensity correlation functions, $g^{(2)}(\tau) - 1$, were measured at a fixed sample position and a scattering angle. Reprinted with permission from [87]. Copyright 2007 by the American Physical Society. **b** Position-dependent intensity correlation functions were observed in a PNIPAM gel at a temperature below its LCST [64]. Reprinted (adapted) with permission from [64]. Copyright 2003 American Chemical Society

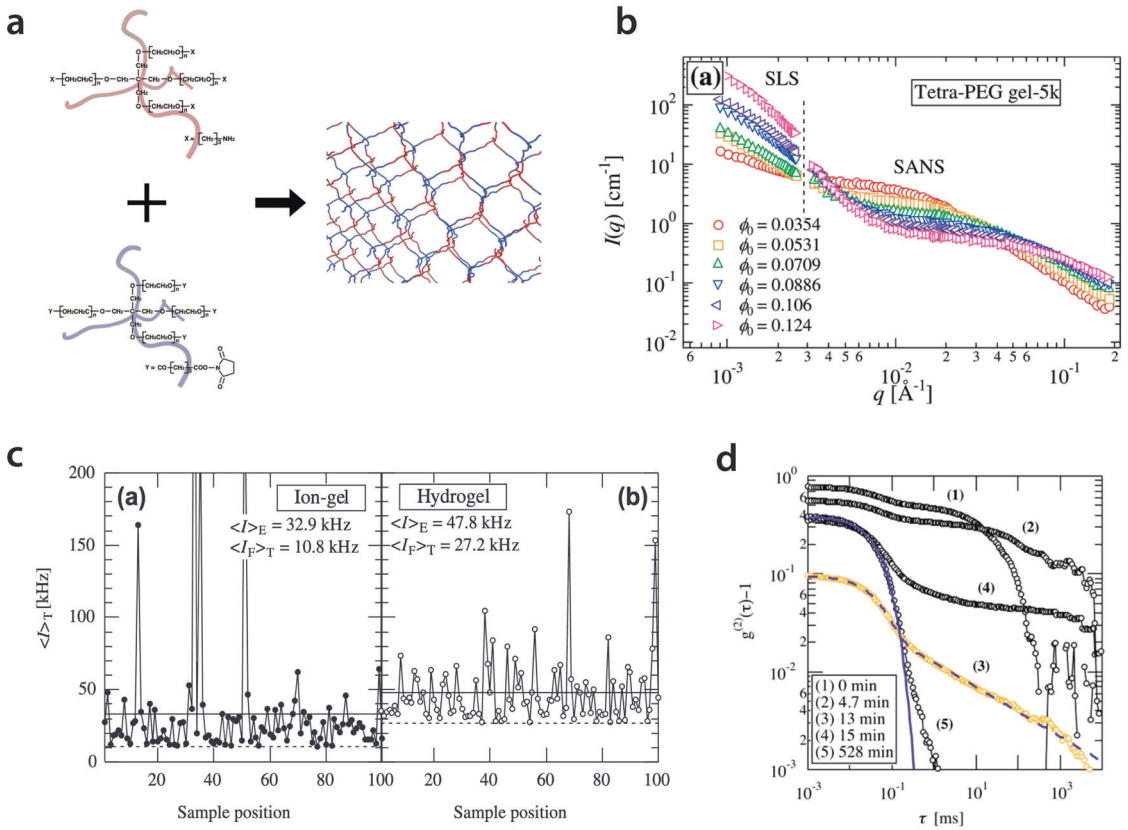

Fig. 4 Near-ideal gel networks synthesized by A–B type end-crosslinking of mutually reactive four-armed polyethylene glycols [40, 71]. **a** The schematic of the tetra-PEG gel [104]. **b** Scattering intensity profiles of tetra-PEG gels synthesized at different polymer volume fractions (ϕ) in aqueous buffer [73]. The scattering intensity was measured using static light scattering (SLS) and small-angle neutron scattering (SANS). Reprinted (adapted) with permission from [71, 73]. Copyright 2009 American Chemical Society. **c** 1D laser speckle patterns of the tetra-PEG gels synthesized in an ionic liquid (left) and water (right) [99]. **d** DLS intensity time correlation function of the tetra-PEG gel during its gelation reaction [99]. The gel used for DLS was synthesized in aqueous buffer. Reprinted from [99] with permission from Elsevier

conventional gels [71, 98]. However, fractal small-angle scattering was observed by light scattering experiments, which cover a length scale of 100 nm–1 μm (Fig. 4b) [73], indicating that spatial defects with a size larger than a few hundred nanometers exist in the tetraPEG gels. The fluctuating 1D laser speckle pattern of the tetraPEG gels also suggests a certain amount of *frozen* spatial heterogeneity in the gel network (Fig. 4c) [99]. The formation of heterogeneous clusters and their immobilization were also observed in tetraPEG gel (Fig. 4d) [99].

Movable crosslinkers

Figure 5 shows a unique polymer gel with movable crosslinkers, known as slide ring gels [72]. The linear polymer chains were tied up together by a pair of connected rings in the shape of the number 8. The ends of the linear polymers are capped with large molecules to prevent the rings from slipping out from the chains. The rings can slide through the polymer chains even after the gel network forms; therefore, the movable crosslinkers enable the local rearrangement of the gel network and reduce the nonuniform distribution of polymer chains formed by the stochastic crosslinking reaction. The mechanical properties of the gels were drastically improved by the movable crosslinkers [9]. The gels can be stretched to more than ten times their original length. However, scattering experiments revealed that a certain amount of spatial heterogeneity exists even in these gels (Fig. 5b, c) [100]. Similar heterogeneous cluster formation and immobilization were observed in the DLS intensity correlation functions (Fig. 5d) [100].

Bond percolation condition

Instead of improving the crosslinking reaction as performed in previous studies, we chose a different direction to achieve homogeneous gels [75]. We focused on the packing conditions of the polymer chains in the pregel solution. We brought a geometric constraint into the polymer chains so

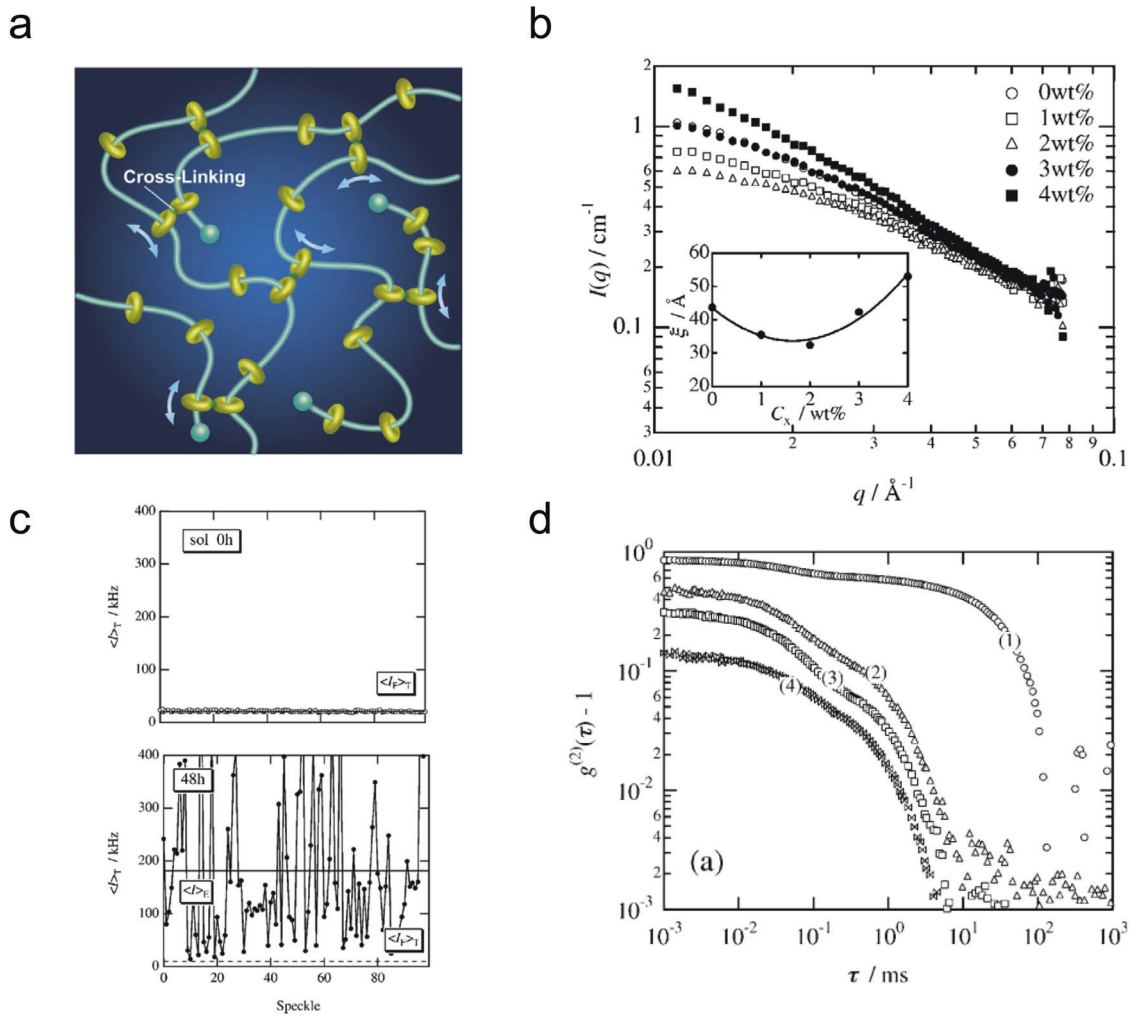

Fig. 5 Rearrangeable gel network synthesized by crosslinking PEG with movable crosslinkers. **a** Schematic of the slide ring gels [105]. **b** Small-angle neutron scattering profile of the slide ring gels in 1 N NaOD [100]. The crosslinking densities were changed in a range of 0–4 wt%. **c** 1D laser speckles in a noncrosslinked slide ring polymer solution (top) and the corresponding slide ring gel (bottom) [100]. **d** DLS intensity correlation functions of a slide ring gel during gelation: (1) sol, (2) gel 4.3 h (gel point), (3) gel 21 h, and (4) gel 48 h [100]. The timestamp denotes the time elapsed from the synthesis

that the polymer solution was always uniformly filled with the starting polymer units throughout the gelation reaction. Our strategy was based on the "bond-percolation" model [77], which is a classical percolation model [29]. The bond percolation model divides the space of the polymer solution into a collection of small sites. The model assumes that mutually exclusive polymer units prepack all these sites, and the crosslinking reaction occurs between nearby units. The polymer units may exchange their positions in the gelation reaction, but the polymer units always pack all the sites throughout the gelation reaction. As long as the polymer units are exclusive, i.e., they do not allow other polymer units to interpenetrate their occupied sites, a highly ordered, ideal network structure is expected to form.

There are four essential points to achieve perfect bond percolation conditions. First, multiarmed star polymers, e.g., tetraPEG, were used as a space-filling unit (Fig. 6a). The multiarmed star polymers show a strong excluded volume effect to prevent other polymer units from interpenetrating into their own pervaded volume. Second, the polymers were dissolved at a concentration higher than its chain overlapping limit, c^*. The optimally crowded condition ensures that the polymer units uniformly fill up the space. When the polymer concentration is too high, entanglements between the polymer units may result in a nonuniform spatial polymer distribution. Third, a solvent with an excellent affinity for the polymer units was used. A low affinity between the solvent and polymer may result in polymer aggregates, which breaks the bond percolation conditions, i.e., one site, one polymer unit. Finally, a fine syringe filter was used to remove dust and nanobubbles from the solution as much as possible. Impurities disturb the

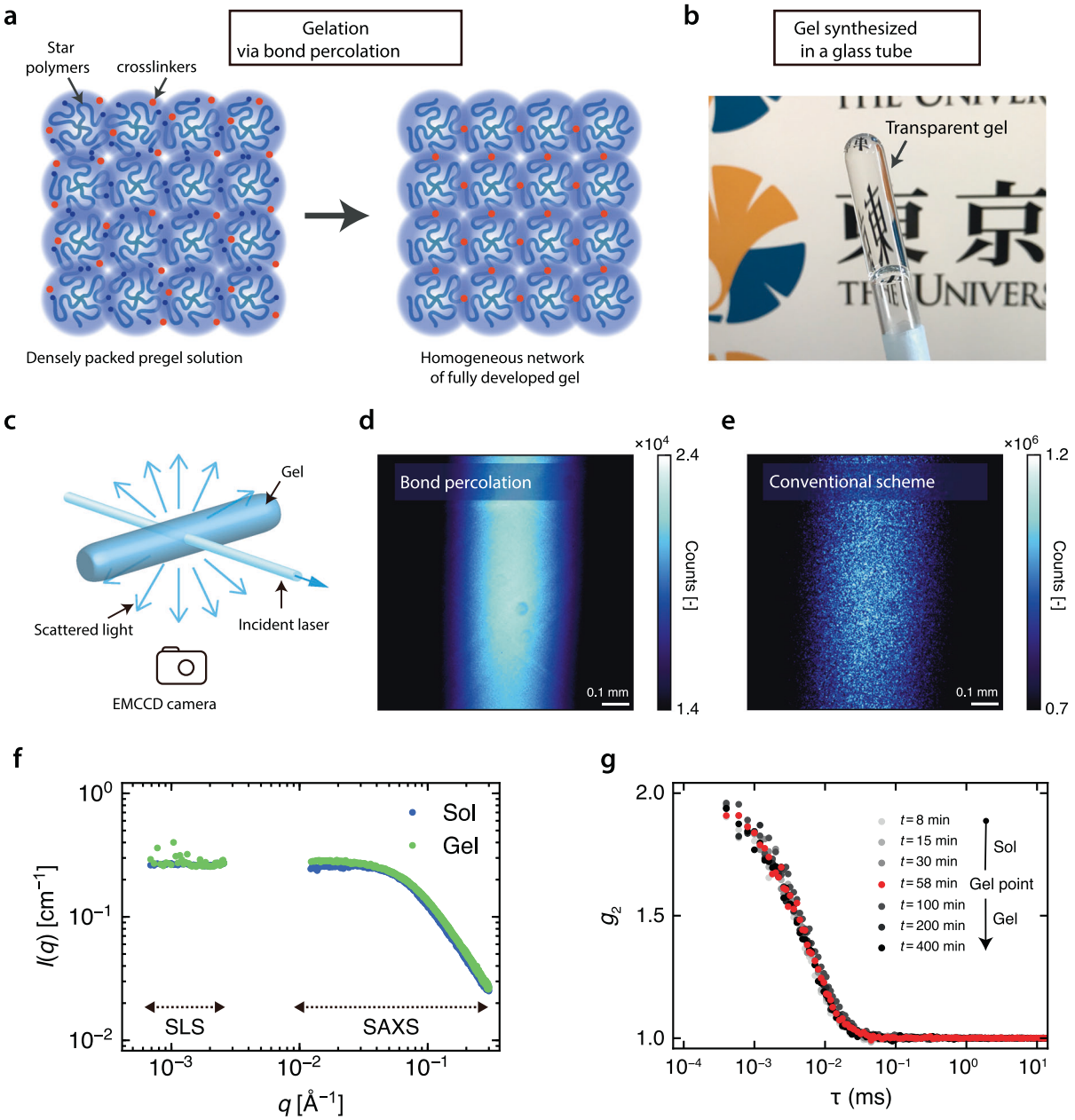

Fig. 6 Highly homogeneous gels synthesized via bond percolation [75]. **a** Schematic of gel synthesis under bond percolation conditions. **b** A photo of the gel synthesized in a glass tube. **c** Schematic of the 2D laser speckle imaging system. **d** 2D laser speckle image of the bond percolation gel. **e** 2D laser speckle image of a gel synthesized by conventional radical polymerization. **f** Scattering profiles of the bond percolation gel and the uncrosslinked polymer solution (sol) by static light scattering (SLS) and SAXS. **g** Intensity correlation functions of the bond percolation gel during gelation. The correlation functions were measured at a fixed scattering angle of 90° by DLS. The red marks show the intensity correlation function at the gel point. The gel point was determined as the point where the storage modulus and loss modulus crossed during dynamic viscoelasticity measurement

proper packing of polymer units. Although all these suggestions had already been mentioned separately in previous studies, they had not been resolved altogether.

We synthesized gels by crosslinking tetraPEG with active ester end groups with a small bifunctional cross-linker, 1,14-diamino-3,6,9,12-tetraoxatetradecane (amino-PEG4-amine), in dehydrated acetonitrile, which is a good solvent for PEG. The solvent quality was determined by confirming no aggregation formation in the pregel solution using DLS. Detailed information for the gel synthesis and DLS test is described in our previous articles [75, 76]. Figure 6b shows the synthesized "bond percolation" gel in a glass tube. We measured the 2D laser speckles of the gels by using a custom-made laser speckle imaging microscope

(Fig. 6c). No stationary laser speckles were observed in the "bond percolation" gel (Fig. 6d), indicating the high homogeneity of the bond percolation gel. In contrast, numerous bright and dark spots, i.e., laser speckles, were observed in the conventional gels (Fig. 6e). Figure 6f shows the scattering profiles of the bond percolation gel and the corresponding uncrosslinked polymer solution (sol). The scattering profiles of the gel and sol overlap each other well, and fractal scattering at small q values ($q << 0.1$ Å^{-1}) was not observed (Fig. 6f). The perfect consistency between the gel and sol profiles at small q values suggests that no spatial heterogeneities existed in the bond percolation gel. There are a few studies showing similar no excess scattering profiles for gels, but the no excess scattering region was limited in the q-range of typical SAXS and SANS setups ($q > 5 \times 10^{-3}$ Å^{-1}) and only for sparsely crosslinked gels [84]. In contrast, in Fig. 6f, we exhibited, for the first time, no excess scattering even in the light scattering region, $q > 5 \times 10^{-4}$ Å^{-1}, and at a high crosslinking ratio. Figure 6g shows the intensity correlation functions (g_2) of the bond percolation gel during its gelation process. Note that g_2, $g^{(2)}(\tau)$, and $G(t)$ are all notations for intensity correlation functions. All g_2 curves fell on a single relaxation curve; there was no change in the intensity correlation functions in the bond percolation gel regardless of the extent of crosslinking, even at the gel point. The gel point of the bond percolation gel was separately determined by a dynamic viscoelasticity measurement. We used the cross point of the storage modulus and the loss modulus of the sample as the gel point. The scattering profiles of a homogeneous gel are very simple and entirely different from those of any other gel, as introduced above.

When the bond percolation breaks

To confirm the importance of the assumptions we made for the ideal bond percolation condition, we deliberately changed the packing state of the polymer units in the pregel solutions (Fig. 7a–c). We used the same star polymers but lowered the polymer concentration below c^* (Fig. 7b) or reduced the solvent affinity (Fig. 7c). The low polymer concentration condition is an underfilled state, where gelation proceeds by site percolation or site-bond percolation. Gel networks containing nanovoids are expected to be formed in the underfilled state (Fig. 7e). In contrast, the low-affinity solvent condition will result in polymer aggregates. Although the polymer units fill all the sites in the pregel solution, some sites will be overfilled with multiple polymer units (Fig. 7c). We refer to the overfilled condition as the "nonideal bond percolation" condition. We used water as the low-affinity solvent for the PEG star polymers. Gel networks with locally dense regions are expected to form under this packing condition (Fig. 7f). Panels g–i in Fig. 7 show the corresponding 2D laser speckle images of the gels synthesized under bond percolation, site percolation, and nonideal bond percolation conditions. Bright and dark interference spots were observed exclusively in the site and nonideal bond percolation gels, suggesting the presence of spatial defects in these gels, as we expected. We can quantitatively assess the extent of the spatial distribution by measuring the polymer dynamics. While all $g^{(2)}{}_{\mathcal{T}}(\tau) - 1$ curves of the bond percolation gel overlap well with each other, the $g^{(2)}{}_{\mathcal{T}}(\tau) - 1$ curves of the site percolation and nonideal bond percolation gels vary, depending on the sample positions. This result suggests the presence of frozen spatial heterogeneities in the nonbond-percolation gels. $g^{(2)}{}_{\mathcal{T}}(\tau) - 1$ did not start from 1 due to the instrumentation factors [101]. For the site percolation and nonideal percolation gels, the ensemble-averaged intensity correlation functions $g^{(2)}{}_{\mathrm{E}}(\tau) - 1$ did not fully relax even at the long lag time, indicating the presence of "frozen" heterogeneities in the gels. The "frozen" spatial defects in the site percolation gel should be voids, which do not fluctuate with time. By contrast, the "frozen" spatial defects in the nonideal bond percolation gel should be local aggregates trapped in the gel network.

To identify the size and volume fraction of the defects in each gel, we further analyzed the gels using SLS and SAXS. Figure 8 shows the normalized scattering profiles of three different gels [76]. The scattering intensity $I(q)$ and scattering vector q are corrected based on the Ornstein–Zernike (OZ) model to normalize the contribution of the concentration fluctuations on the scattering profiles [102, 103]. While the region $q\xi > 1$ corresponds to a length scale that is smaller than the size of the concentration fluctuation, the region $q\xi < 1$ shows a spatial correlation longer than the screening length of the concentration fluctuation. The scattering curves for all three gels overlap with each other when $q\xi > 1$, suggesting successful normalization. The solid curves show good fitting using the OZ model function, which describes the scattering originating from concentration fluctuations of semidilute polymer chains. While the single OZ function can reproduce the normalized scattering profiles of the bond percolation gel, the scattering profiles of the site percolation and nonideal bond percolation gels deviated from the OZ curves at small q values ($q\xi < 1$). The consistency between the scattering profile and OZ function indicates that no additional spatial correlations are formed by gelation. In contrast, the profiles that deviated from the OZ function suggest the presence of spatial heterogeneities.

In previous studies, the type of spatial heterogeneity was hard to determine because both sparse regions (voids) and dense regions (aggregates) tend to be formed during the gelation process. However, as we started from a highly homogeneous gel and deliberately deviated the packing

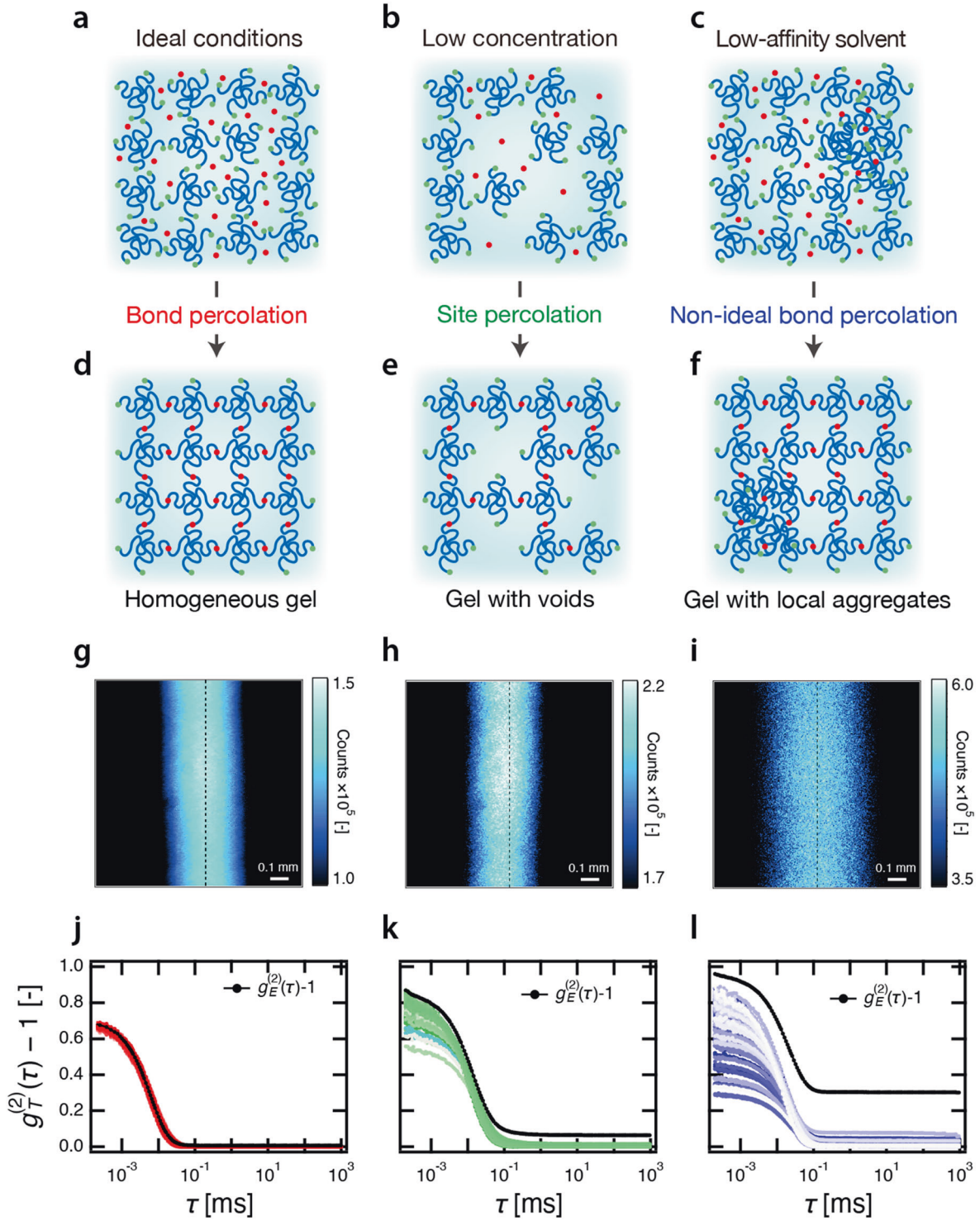

Fig. 7 Gels synthesized with the same star polymers at different polymer concentrations and solvent qualities [76]. **a**–**c** Schematics of three pregel solutions to induce different percolation processes, and **d**–**f** the expected structures of the resulting gels: **a**, **d** bond percolation condition, **b**, **e** site percolation condition, **c**, **f** nonideal bond percolation condition. **g**–**i** 2D laser speckle images of bond percolation, site percolation, and nonideal percolation gels. **j**–**l** Intensity correlation functions ($g^{(2)}{}_T(\tau) - 1$) at 100 different sample positions for the corresponding gels by DLS measurements. The black circles with lines are the ensemble average intensity correlation functions, $g^{(2)}{}_E(\tau) - 1$. Reprinted (adapted) with permission from [76]. Copyright 2020 American Chemical Society

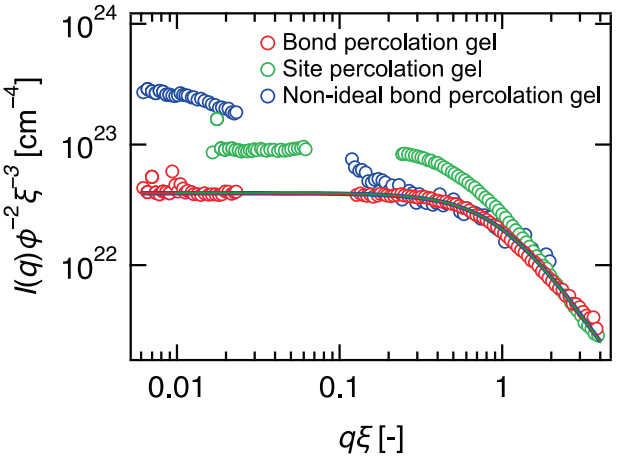

Fig. 8 SAXS profiles of three different gels synthesized by different percolation conditions [76]. $I(q)$ and q are corrected based on the Ornstein–Zernike (OZ) model to normalize the contribution of the concentration fluctuations. The solid curves show the fittings with the OZ model. The scattering profiles deviating from the OZ curves at $q\xi < 1$ indicate spatial correlations from spatial defects in the gels. Reprinted (adapted) with permission from [76]. Copyright 2020 American Chemical Society

conditions of the prepolymers, we could estimate the type of spatial heterogeneity in these gels well. The typical sizes of these spatial heterogeneities were estimated using the Guinier equation, which is a versatile equation to calculate the z-average gyration radius of objects with arbitrary shapes. The size of the spatial heterogeneities, i.e., nanovoids, in the site percolation gel was estimated to be $R_g = 7.1$ nm, approximately twice the star polymer units, $R_g = 3.5$ nm. The total volume fraction of the spatial heterogeneities was roughly estimated to be ~26 vol% determined from the scattering intensity of the heterogeneities. In contrast, the heterogeneities size in the nonideal bond percolation gel was ~54 nm, which is much larger than the size of the polymer units. The volume fraction of the aggregates was estimated to be ~5 vol%, and the local concentration of the aggregates was only 10% higher than the polymer concentration in the gel network. In the nonideal bond percolation gel, large but very loose aggregates were trapped in the gel network.

Summary and future perspective

Our findings demonstrate that the heterogeneity may not be an inherent nature of the gels. The scattering profiles from the bond percolation gel established a new benchmark for future gel structure analysis. The key point in fabricating homogeneous gels lies in the packing state of the polymers in the pregel solution. The simplicity of our gel preparation scheme will enable us to synthesize homogeneous gels with a highly ordered network from a variety of polymers with different chemical structures and functionalities, which will lead to a wide range of new applications.

Acknowledgements The author would like to express his gratitude to all his colleagues for their valuable contributions to this focus review. The author is deeply indebted to Prof. Mitsuhiro Shibayama (Comprehensive Research Organization for Science and Society) and Prof. Takamasa Sakai (University of Tokyo) for their continuous encouragement and constructive discussions. This research was supported by JSPS KAKENHI grants JP17K14536 and JP19K15628, Eno Scientific Foundation, the University of Tokyo Gap Fund Program, and the Japan Science and Technology Agency (JST) to T.S. (CREST Grant JPMJCR1992).

Compliance with ethical standards

Conflict of interest The author declares no competing interests.

Publisher's note Springer Nature remains neutral with regard to jurisdictional claims in published maps and institutional affiliations.

References

1. Baldock C, Deene YD, Doran S, Ibbott G, Jirasek A, Lepage M, et al. Polymer gel dosimetry. Phys Med Biol. 2010;55:R1–63.
2. Hoffman AS. Hydrogels for biomedical applications. Adv Drug Deliv Rev. 2012;64:18–23.
3. Yang C, Suo Z. Hydrogel ionotronics. Nat Rev Mater. 2018;3:125–42.
4. Kamata H, Li X, Chung U, Sakai T. Design of hydrogels for biomedical applications. Adv Healthc Mater. 2015;4:2360–74.
5. Hayashi K, Okamoto F, Hoshi S, Katashima T, Zujur DC, Li X, et al. Fast-forming hydrogel with ultralow polymeric content as an artificial vitreous body. Nat Biomed Eng. 2017;1:0044.
6. Shibayama M, Li X, Sakai T. Gels: From Soft Matter to Bio-Matter. Ind Eng Chem Res. 2017;57:1121–8.
7. Mezzenga R, Schurtenberger P, Burbidge A, Michel M. Understanding foods as soft materials. Nat Mater. 2005;4:729–40.
8. Sun JY, Zhao X, Illeperuma WR, Chaudhuri O, Oh KH, Mooney DJ, et al. Highly stretchable and tough hydrogels. Nature. 2012;489:133–6.
9. Jiang L, Liu C, Mayumi K, Kato K, Yokoyama H, Ito K. Highly stretchable and instantly recoverable slide-ring gels consisting of enzymatically synthesized polyrotaxane with low host coverage. Chem Mater. 2018;30:5013–9.
10. Tang J, Katashima T, Li X, Mitsukami Y, Yokoyama Y, Sakumichi N, et al. Swelling behaviors of hydrogels with alternating neutral/highly charged sequences. Macromolecules. 2020;53:8244–54.
11. Fujiyabu T, Li X, Chung U, Sakai T. Diffusion behavior of water molecules in hydrogels with controlled network structure. Macromolecules. 2019;52:1923–9.
12. Fujiyabu T, Li X, Shibayama M, Chung U, Sakai T. Permeation of water through hydrogels with controlled network structure. Macromolecules. 2017;50:9411–6.
13. Li X, Khairulina K, Chung U, Sakai T. Electrophoretic mobility of double-stranded DNA in polymer solutions and gels with tuned structures. Macromolecules. 2014;47:3582–6.
14. Khairulina K, Li X, Nishi K, Shibayama M, Chung U, Sakai T. Electrophoretic mobility of semi-flexible double-stranded DNA in defect-controlled polymer networks: Mechanism investigation

and role of structural parameters. J Chem Phys. 2015;142:234904.
15. Li X, Khairulina K, Chung U, Sakai T. Migration behavior of rodlike dsDNA under electric field in homogeneous polymer networks. Macromolecules. 2013;46:8657–63.
16. Kureha T, Hayashi K, Li X, Shibayama M. Mechanical properties of temperature-responsive gels containing ethylene glycol in their side chains. Soft Matter. 2020;16:10946–53.
17. Kureha T, Hayashi K, Ohira M, Li X, Shibayama M. Dynamic fluctuations of thermoresponsive poly(oligo-ethylene glycol methyl ether methacrylate)-based hydrogels investigated by dynamic light scattering. Macromolecules. 2018;51:8932–9.
18. Shibayama M, Tanaka T. Volume phase-transition and related phenomena of polymer gels. Adv Polym Sci. 1993;109:1–62.
19. Addad JPC. Physical Properties of Polymeric Gels. New York: Wiley; 1996.
20. Sakai T. Physics of Polymer Gels. (2020). https://doi.org/10.1002/9783527346547.
21. Takashima R, Ohira M, Yokochi H, Aoki D, Li X, Otsuka H. Characterization of N -phenylmaleimide-terminated poly(ethylene glycol)s and their application to a tetra-arm poly(ethylene glycol) gel. Soft Matter. 2020;16:10869–75.
22. Huang X, Nakagawa S, Li X, Shibayama M, Yoshie N. A simple and versatile method for the construction of nearly ideal polymer networks. Angew Chem Int Ed. 2020;59:1–8.
23. Tsuji Y, Li X, Shibayama M. Evaluation of mesh size in model polymer networks consisting of tetra-arm and linear poly(ethylene glycol)s. Gels. 2018;4:50.
24. Li X, Watanabe N, Sakai T, Shibayama M. Probe diffusion of sol–gel transition in an isorefractive polymer solution. Macromolecules. 2017;50:2916–22.
25. Osada Y, Kajiwara K, Fushimi T, Irasa O, Hirokawa Y, Matsunaga T, et al. Gels Handbook. 1. San Diego: Elsevier; 2001.
26. Adibnia V, Hill RJ. Universal aspects of hydrogel gelation kinetics, percolation and viscoelasticity from PA-hydrogel rheology. J Rheol. 2016;60:541–8.
27. Okay O. Kinetics of gelation in free radical crosslinking copolymerization. Polymer. 1994;35:2613–8.
28. Watanabe N, Li X, Shibayama M. Probe diffusion during sol–gel transition of a radical polymerization system using isorefractive dynamic light scattering. Macromolecules. 2017;50:9726–33.
29. Stauffer D, Aharony A. Introduction To Percolation Theory. Taylor & Francis; 1994. https://doi.org/10.1201/9781315274386.
30. Li X, Noritomi T, Sakai T, Gilbert EP, Shibayama M. Dynamics of critical clusters synthesized by end-coupling of four-armed poly(ethylene glycol)s. Macromolecules. 2019;52:5086–94.
31. Fujiyabu T, Toni F, Li X, Chung U, Sakai T. Three cooperative diffusion coefficients describing dynamics of polymer gels. Chem Commun. 2018;59:5151.
32. Teraoka I. Polymer Solutions. John Wiley & Sons, Inc.; 2002. https://doi.org/10.1002/0471224510.
33. Shibayama M. Spatial inhomogeneity and dynamic fluctuations of polymer gels. Macromol Chem Phys. 1998;199:1–30.
34. Lorenzo FD, Seiffert S. Nanostructural heterogeneity in polymer networks and gels. Polym Chem. 2015;6:5515–28.
35. Denisin AK, Pruitt BL. Tuning the range of polyacrylamide gel stiffness for mechanobiology applications. ACS Appl Mater Interfaces. 2016;8:21893–902.
36. Hiroi T, Okazumi Y, Littrell KC, Narita Y, Tanaka N, Shibayama M. Mechanism of heat-induced gelation for ovalbumin and its N-terminus cleaved form. Polymer. 2016;93:152–8.
37. Matsuo ES, Tanaka T. Patterns in shrinking gels. Nature. 1992;358:482–5.
38. Ohira M, Li X, Gupit CI, Kamata H, Sakai T, Shibayama M. Dynamics of thermoresponsive conetwork gels composed of poly(ethylene glycol) and poly(ethyl glycidyl ether-co-methyl glycidyl ether). Polymer. 2018;155:75–82.
39. Tamate R, Hashimoto K, Li X, Shibayama M, Watanabe M. Effect of ionic liquid structure on viscoelastic behavior of hydrogen-bonded micellar ion gels. Polymer. 2019;178:121694.
40. Shibayama M, Li X, Sakai T. Precision polymer network science with tetra-PEG gels—a decade history and future. Colloid Polym Sci. 2018;297:1–12.
41. Morishima K, Li X, Oshima K, Mitsukami Y, Shibayama M. Small-angle scattering study of tetra-poly(acrylic acid) gels. J Chem Phys. 2018;149:163301.
42. Nakagawa S, Li X, Shibayama M, Kamata H, Sakai T, Gilbert EP. Insight into the microscopic structure of module-assembled thermoresponsive conetwork hydrogels. Macromolecules. 2018;51:6645–52.
43. Nakagawa S, Li X, Kamata H, Sakai T, Gilbert EP, Shibayama M. Microscopic Structure of the "Nonswellable" Thermoresponsive Amphiphilic Conetwork. Macromolecules. 2017;50:3388–95.
44. Ohira M, Tsuji Y, Watanabe N, Morishima K, Gilbert EP, Li X, et al. Quantitative structure analysis of a near-ideal polymer network with deuterium label by small-angle neutron scattering. Macromolecules. 2020;53:4047–54.
45. Li X, Hirosawa K, Sakai T, Gilbert EP, Shibayama M. SANS study on critical polymer clusters of tetra-functional polymers. Macromolecules. 2017;50:3655–61.
46. Shibayama M, Norisuye T, Nomura S. Cross-link density dependence of spatial inhomogeneities and dynamic fluctuations of poly(N-isopropylacrylamide) Gels. Macromolecules. 1996;29:8746–50.
47. Norisuye T, Tran-Cong-Miyata Q, Shibayama M. Dynamic inhomogeneities in polymer gels investigated by dynamic light scattering. Macromolecules. 2004;37:2944–53.
48. Ikkai F, Shibayama M, Han CC. Effect of degree of cross-linking on spatial inhomogeneity in charged gels. 2. Small-angle neutron scattering study. Macromolecules. 1998;31:3275–81.
49. Roe RJ. Methods of X-ray and Neutron Scattering in Polymer Science. Oxford University Press; 2000.
50. Pecora R. Dynamic Light Scattering. Springer Science & Business Media; 1985. https://doi.org/10.1007/978-1-4613-2389-1.
51. Tanaka M, Sawada T, Li X, Serizawa T. Controlled assembly of filamentous viruses into hierarchical nano- to microstructures at liquid/liquid interfaces. Rsc Adv. 2020;10:26313–8.
52. Gupit CI, Li X, Maekawa R, Hasegawa N, Iwase H, Takata S, et al. Nanostructures and viscosities of nafion dispersions in water/ethanol from dilute to concentrated regimes. Macromolecules. 2020;53:1464–73.
53. Mizuno H, Hashimoto K, Tamate R, Kokubo H, Ueno K, Li X, et al. Microphase-separated structures of ion gels consisting of ABA-type block copolymers and an ionic liquid: A key to escape from the trade-off between mechanical and transport properties. Polymer. 2020;206:122849.
54. Tamate R, Hashimoto K, Horii T, Hirasawa M, Li X, Shibayama M, et al. Self-healing micellar ion gels based on multiple hydrogen bonding. Adv Mater. 2018;100:1802792.
55. Ito A, Yasuda T, Yoshioka T, Yoshida A, Li X, Hashimoto K, et al. Sulfonated polyimide/ionic liquid composite membranes for CO_2 separation: transport properties in relation to their nanostructures. Macromolecules. 2018;51:7112–20.
56. Hashimoto K, Hirasawa M, Kokubo H, Tamate R, Li X, Shibayama M, et al. Transport and mechanical properties of ABA-type triblock copolymer ion gels correlated with their microstructures. Macromolecules. 2019;52:8430–9.
57. Wang C, Hashimoto K, Tamate R, Kokubo H, Morishima K, Li X, et al. Viscoelastic change of block copolymer ion gels in a

photo-switchable azobenzene ionic liquid triggered by light. Chem Commun. 2019;55:1710–3.
58. Morishima K, Nakamura N, Matsui K, Tanaka Y, Masunaga H, Mori S, et al. Formation of clusters in whiskies during the maturation process. J Food Sci. 2019;84:59–64.
59. Mallam S, Horkay F, Hecht AM, Geissler E. Scattering and swelling properties of inhomogeneous polyacrylamide gels. Macromolecules. 1989;22:3356–61.
60. Takata S, Norisuye T, Shibayama M. Small-angle neutron-scattering study on preparation temperature dependence of thermosensitive gels. Macromolecules. 2002;35:4779–84.
61. Ikkai F, Shibayama M. Static inhomogeneities in thermoreversible physical gels. Phys Rev Lett. 1999;82:4946–9.
62. Matsuo ES, Orkisz M, Sun S-T, Li Y, Tanaka T. Origin of structural inhomogeneities in polymer gels. Macromolecules. 1994;27:6791–6.
63. Joosten JGH, McCarthy JL, Pusey PN. Dynamic and static light scattering by aqueous polyacrylamide gels. Macromolecules. 1991;24:6690–9.
64. László K, Kosik K, Rochas C, Geissler E. Phase transition in poly(N-isopropylacrylamide) hydrogels induced by phenols. Macromolecules. 2003;36:7771–6.
65. Panyukov S, Rabin Y. Polymer gels: frozen inhomogeneities and density fluctuations. Macromolecules. 1996;29:7960–75.
66. Pusey PN, Megen WV. Dynamic light scattering by non-ergodic media. Phys A: Stat Mech its Appl. 1989;157:705–41.
67. Shibayama M, Fujikawa Y, Nomura S. Dynamic light scattering study of poly(N-isopropylacrylamide-co-acrylic acid) gels. Macromolecules. 1996;29:6535–40.
68. Rouf-George C, Munch JP, Schosseler F, Pouchelon A, Beinert G, Boue F, et al. Thermal and quenched fluctuations of polymer concentration in poly(dimethylsiloxane) gels. Macromolecules. 1997;30:8344–59.
69. Mark JE, Sullivan JL. Model networks of end-linked polydimethylsiloxane chains. I. Comparisons between experimental and theoretical values of the elastic modulus and the equilibrium degree of swelling. J Chem Phys. 1977;66:1006–11.
70. Ngai T, Wu C, Chen Y. Origins of the speckles and slow dynamics of polymer gels. J Phys Chem B. 2004;108:5532–40.
71. Sakai T, Matsunaga T, Yamamoto Y, Ito C, Yoshida R, Suzuki S, et al. Design and fabrication of a high-strength hydrogel with ideally homogeneous network structure from tetrahedron-like macromonomers. Macromolecules. 2008;41:5379–84.
72. Okumura Y, Ito K. The polyrotaxane gel: a topological gel by figure-of-eight cross-links. Adv Mater. 2001;13:485–7.
73. Matsunaga T, Sakai T, Akagi Y, Chung U, Shibayama M. SANS and SLS studies on tetra-arm PEG gels in as-prepared and swollen states. Macromolecules. 2009;42:6245–52.
74. Karino T, Okumura Y, Ito K, Shibayama M. SANS studies on spatial inhomogeneities of slide-ring gels. Macromolecules. 2004;37:6177–82.
75. Li X, Nakagawa S, Tsuji Y, Watanabe N, Shibayama M. Polymer gel with a flexible and highly ordered three-dimensional network synthesized via bond percolation. Sci Adv. 2019;5:eaax8647.
76. Tsuji Y, Nakagawa S, Gupit CI, Ohira M, Shibayama M, Li X. Selective doping of positive and negative spatial defects into polymer gels by tuning the pregel packing conditions of star polymers. Macromolecules. 2020;53:7537–45.
77. Coniglio A, Stanley HE, Klein W. Site-bond correlated-percolation problem: a statistical mechanical model of polymer gelation. Phys Rev Lett. 1979;42:518–22.
78. Draget KI, Stokke BT, Yuguchi Y, Urakawa H, Kajiwara K. Small-angle X-ray scattering and rheological characterization of alginate gels. 3. Alginic acid gels. Biomacromolecules. 2003;4:1661–8.
79. Susaki EA, Shimizu C, Kuno A, Tainaka K, Li X, Nishi K, et al. Versatile whole-organ/body staining and imaging based on electrolyte-gel properties of biological tissues. Nat Commun. 2020;11:1982.
80. Horkay F, Basser PJ. Ionic and pH effects on the osmotic properties and structure of polyelectrolyte gels. J Polym Sci Part B: Polym Phys. 2008;46:2803–10.
81. Geissler E, Horkay F, Hecht AM. Scattering from network polydispersity in polymer gels. Phys Rev Lett. 1993;71:645–8.
82. Norisuye T, Masui N, Kida Y, Ikuta D, Kokufuta E, Ito S, et al. Small angle neutron scattering studies on structural inhomogeneities in polymer gels: irradiation cross-linked gels vs chemically cross-linked gels. Polymer. 2002;43:5289–97.
83. Horkay F, Basser PJ, Hecht AM, Geissler E. Structural investigations of a neutralized polyelectrolyte gel and an associating neutral hydrogel. Polymer. 2005;46:4242–7.
84. Mendes JE, Lindner P, Buzier M, Boué F, Bastide J. Experimental evidence for inhomogeneous swelling and deformation in statistical gels. Phys Rev Lett. 1991;66:1595–8.
85. Goren C, Rabin Y, Rosenbluh M, Cohen Y. Elastic recovery of gels on mesoscopic length scales. a photon correlation spectroscopy study. Macromolecules. 2000;33:5757–9.
86. Panyukov S, Rabin Y. Statistical physics of polymer gels. Phys Rep. 1996;269:1–131.
87. Matsunaga T, Shibayama M. Gel point determination of gelatin hydrogels by dynamic light scattering and rheological measurements. Phys Rev E Stat Nonlin Soft Matter Phys. 2007;76:030401.
88. Shibayama M. Universality and specificity of polymer gels viewed by scattering methods. B Chem Soc Jpn. 2006;79:1799–819.
89. Nishi K, Fujii K, Katsumoto Y, Sakai T, Shibayama M. Kinetic aspect on gelation mechanism of tetra-PEG hydrogel. Macromolecules. 2014;47:3274–81.
90. Li X, Kondo S, Chung U, Sakai T. Degradation behavior of polymer gels caused by nonspecific cleavages of network strands. Chem Mater. 2014;26:5352–7.
91. Li X, Tsutsui Y, Matsunaga T, Shibayama M, Chung U, Sakai T. Precise control and prediction of hydrogel degradation behavior. Macromolecules. 2011;44:3567–71.
92. Kamata H, Akagi Y, Kayasuga-Kariya Y, Chung UI, Sakai T. "Nonswellable" hydrogel without mechanical hysteresis. Science. 2014;343:873–5.
93. Akagi Y, Gong JP, Chung U, Sakai T. Transition between phantom and affine network model observed in polymer gels with controlled network structure. Macromolecules. 2013;46:1035–40.
94. Fujii K, Asai H, Ueki T, Sakai T, Imaizumi S, Chung U, et al. High-performance ion gel with tetra-PEG network. Soft Matter. 2012;8:1756–9.
95. Sakai T, Akagi Y, Matsunaga T, Kurakazu M, Chung U, Shibayama M. Highly elastic and deformable hydrogel formed from tetra-arm polymers. Macromol Rapid Commun. 2010;31:1954–9.
96. Fujinaga I, Yasuda T, Asai M, Chung U, Katashima T, Sakai T. Cluster growth from a dilute system in a percolation process. Polym J. 2019;1–9. https://doi.org/10.1038/s41428-019-0279-z.
97. Ikeda T. Preparation of (2 × 4)-type tetra-PEG ion gels through Cu-free azide–alkyne cycloaddition. Polym J. 2020;1–7. https://doi.org/10.1038/s41428-020-0363-4.
98. Akagi Y, Katashima T, Sakurai H, Chung U, Sakai T. Ultimate elongation of polymer gels with controlled network structure. Rsc Adv. 2013;3:13251.
99. Asai H, Nishi K, Hiroi T, Fujii K, Sakai T, Shibayama M. Gelation process of Tetra-PEG ion-gel investigated by time-resolved dynamic light scattering. Polymer. 2013;54:1160–6.
100. Shibayama M, Karino T, Domon Y, Ito K. Complementary use of small-angle neutron scattering and dynamic light scattering

studies for structure analysis and dynamics of polymer gels. J Appl Crystallogr. 2007;40:S43–7.
101. Rochas C, Geissler E. Measurement of dynamic light scattering intensity in gels. Macromolecules. 2014;47:8012–7.
102. Gennes PGde. Scaling Concepts in Polymer Physics. New York: Cornell University Press; 1979.
103. Horkay F, Nishi K, Shibayama M. Decisive test of the ideal behavior of tetra-PEG gels. J Chem Phys. 2017;146:164905-1–8.
104. Fujiyabu T, Yoshikawa Y, Chung U, Sakai T. Structure-property relationship of a model network containing solvent. Sci Technol Adv Mat. 2019;20:608–21.
105. Noda Y, Hayashi Y, Ito K. From topological gels to slide-ring materials. J Appl Polym Sci. 2014;131:4059.

Xiang Li is currently an Assistant Professor in the Yamamuro Lab, Neutron Science laboratory in the Institue for Solid State Physics, University of Tokyo. He was a Ph.D. student under the supervision of Prof. Takamasa Sakai at the Department of Bioengineering, University of Tokyo. After obtaining his Ph.D. degree in engineering in 2015, he joined the Shibayama lab in the current institute as an Assistant Professor to study polymers' nanostructure. From 2020, he joined the Yamamuro Lab as an Assistant Professor and started researches for nanoseconds dynamics of polymers. His scientific focus is on understanding polymer structure and dynamics in solutions, gels, and elastomers. He employs a combination of scattering techniques (neutron, X-ray, and light) and rheological measurements to reveal the underlying mechanism between nanostructures and macroscopic mechanical response.